Application of microbubble air flotation to harvest Microcystis sp. from agriculture wastewater: the regulation and mechanisms

hui liu[1], Jianfeng Ye[2], Zhihao Zhu[3], Zhaofeng Song[1], Huiting Xu[1], and Tianchen Xu[1]

[1]Shanghai Academy of Environmental Sciences
[2]Tongji University College of Environmental Science and Engineering
[3]Shanghai Ocean University999 Hucheng Ring Rd

March 23, 2024

Abstract

The harvesting of microalgae is the main bottleneck of its large-scale biomass production, and seeking an efficient, green, and low-cost microalgae harvesting technology is one of the urgent problems to be solved. Microbubble air flotation has been proved to be an effective measure, but the generation of the right size of microbubbles and the mechanism of microbubbles-algal cells attachment are still unclear. In this study, microbubble air flotation was used as a harvesting method for *Microcystis* cultured in agricultural wastewater. The process mechanism of microbubble air flotation harvesting microalgae in wastewater was fully revealed from three aspects (the design of bubble formation, the adhesion law, and the recovery rate of microalgae under different working conditions). The results show that the length of the release pipe is the main factor affecting the proportion of microbubbles with particle size less than 50 μm. In the process of adhesion, when the particle size of microbubbles is 0.6˜1.7 times the size of *Microcystis*, the adhesion efficiency of microbubbles to *Microcystis* is the highest. Under the conditions of pressure 0.45 MPa, gas-liquid ratio 5% and release pipe length 100 cm, the harvesting performance of *Microcystis* was the best. Microbubble air flotation has better harvesting performance of *Microcystis* with higher density. By understanding the mechanism of microbubble flotation, the technical parameters of microbubble flotation for harvesting energy microalgae are optimized to provide support for the development of efficient and low-cost devices and equipment for collecting microalgae.

Application of microbubble air flotation to harvest *Microcystis* sp. from agriculture wastewater: the regulation and mechanisms

Jianfeng Ye[a,b], Zhihao Zhu[c], Zhaofeng Song[d], Huiting Xu[d], Tianchen Xu[d], Hui Liu[d,*]

([a] *College of Environmental Science and Engineering,Tongji University, 1239 Siping Rd., 200092, Shanghai, China.*

[b] *State Key Laboratory of Pollution Control and Resource Reuse,Tongji University, 1239 Siping Rd., 200092, Shanghai, China.*

[c] *College of Marine Ecology and Environment, Shanghai Ocean University,999 Hucheng Ring Rd., 201306, Shanghai, China.*

[d] *Water Research Institute, Shanghai Academy of Environmental Sciences, 508 Qinzhou Rd, 200233 Shanghai, China.*)

* Corresponding author

E-mail: lhsaes@163.com

Tel.: 86-21-64085119

Abstract

The harvesting of microalgae is the main bottleneck of its large-scale biomass production, and seeking an efficient, green, and low-cost microalgae harvesting technology is one of the urgent problems to be solved. Microbubble air flotation has been proved to be an effective measure, but the generation of the right size of microbubbles and the mechanism of microbubbles-algal cells attachment are still unclear. In this study, microbubble air flotation was used as a harvesting method for *Microcystis* cultured in agricultural wastewater. The process mechanism of microbubble air flotation harvesting microalgae in wastewater was fully revealed from three aspects (the design of bubble formation, the adhesion law, and the recovery rate of microalgae under different working conditions). The results show that the length of the release pipe is the main factor affecting the proportion of microbubbles with particle size less than 50 μm. In the process of adhesion, when the particle size of microbubbles is 0.6˜1.7 times the size of *Microcystis* , the adhesion efficiency of microbubbles to *Microcystis* is the highest. Under the conditions of pressure 0.45 MPa, gas-liquid ratio 5% and release pipe length 100 cm, the harvesting performance of*Microcystis* was the best. Microbubble air flotation has better harvesting performance of *Microcystis* with higher density. By understanding the mechanism of microbubble flotation, the technical parameters of microbubble flotation for harvesting energy microalgae are optimized to provide support for the development of efficient and low-cost devices and equipment for collecting microalgae.

Keywords:Microcystis, Microbubble flotation, Agricultural wastewater, Mechanisms

1.Introduction

With the gradual depletion of fossil energy and the environmental pollution caused by the exploitation and utilization of fossil energy, finding clean and renewable new energy is an urgent problem to be solved in today's field (Yoro et al., 2021). Energy microalgae, as a renewable biomass energy source, has become a hot spot because of its short growth cycle, large biomass per unit area and strong environmental adaptability (Peter et al., 2022; Siddiki et al., 2022). In the process of cultivating energy microalgae, it is necessary to provide growth elements including water, inorganic nutrients and CO_2, whose cultivation cost accounts for more than 70% of the total cost of microbial diesel production (Rawat et al., 2011), which restricts the development of microalgae biomass energy technology. However, China, as the largest livestock breeding and consumer in the world (Aravani et al., 2022), with a large amount of aquaculture wastewater with high nitrogen and phosphorus content, the microalgae photosynthetic bioreactor was introduced into the microalgae photosynthetic bioreactor as the medium for energy microalgae after preliminary treatment, which could synergistic achieve the goal of deep purification of aquaculture wastewater and reduction of the culture cost of microalgae biomass energy (Lopez-Sanchez et al., 2022). However, from the perspective of large-scale production of energy microalgae, separation from the aqueous growth medium is difficult and cost as microalgae are small (3˜30 μm) in dilute suspension, and have a specific gravity similar to that of their medium (Ali et al., 2021). In the energy microalgae industry chain, the cost consumed in the harvesting process accounts for about 20%˜30% of the whole cultivation cost of microalga (Rawat et al., 2011). Therefore, considering the impact of energy microalgae harvesting technology on oil extraction and subsequent finishing operation, the method must not contaminate the biomass or create atoxic medium for recycle (Uduman et al., 2010).

At present, the harvesting technologies of energy microalgae mainly include centrifugation, flocculation, filtration, traditional air flotation, etc. (Zhou et al., 2021). Most current harvesting methods have either economic or technical limitations, which include high energy costs, flocculant toxicity, or non-feasible scale-up (Fasaei et al., 2018; Fuad et al., 2018; Laamanen et al., 2021; Oh et al., 2001; Rawat et al., 2013). Flotation recently emerging as a promising alternative based on its good scale-up potential due to technical and economic parameters, such as lower energy and maintenance costs. Traditionally flotation is done either by air addition through a diffuser (dispersed air flotation) or through pressurization (dissolved air flotation) (Aulenbach et al., 2010). Dissolved air flotation separation is more efficient than dispersed air flotation, is more commonly used, and is also proven on a large scale (Christenson & Sims, 2011).The traditional air flotation method requires the addition of chemical flocculant (Laamanen et al., 2021), which has a good

harvesting effect, but has a high cost. Moreover, the quality of energy microalgae will decrease due to the cytolysis caused by aluminum salt (Teixeira et al., 2010).

It has been shown that smaller bubbles result in higher capture efficiency (Hanotu et al., 2012). Molina et al. present possibly the closest technique to micro-flotation for algal harvesting (Molina et al., 2003). One of the efficient ways of facilitating bubble–particle interaction in the liquid rather than merely passing the bubbles through the liquid without it adhering and lifting the particles out of solution, is to generate the right size of microbubbles. The operational parameters such as pressure, gas/liquid ratio, and set-up of the release pipe can affect the size of microbubbles. So far, studies on microalgae microbubbles flotation have mainly focused on the optimization of conditions, including hydraulic loading rate, initial algal concentration, air to solids ratio, pH, salinity, and the type of flotation. However, the mechanism of micro flotation for harvesting energy microalgae has not been revealed. The harvesting performance of the flotation process depends on the attachment of microalgae cells onto microbubbles. Therefore, a solid understanding of the attachment mechanism is necessary to perform this harvesting operation.

This work is aimed at performing an experimental investigation of the interactions between microalgae cells and microbubbles to gain a deep insight into the mechanism governing microalgae cell to microbubbles attachment in the flotation process. The morphological characteristics and motion law of microbubbles under different operational parameters were analyzed, and the response relationship between the particle size of microbubbles and the energy microalgae was clarified. The technical parameters of harvesting energy microalgae by microbubble air flotation were optimized to provide a basis for the application of microbubble air flotation harvesting technology in microalgae industrialization.

2.Material and Methods

2.1. Wastewater and Microalgae species

The microalgae selected in this study was *Microcystis sp* .. The effluent from anaerobic fermentation tank of a pig factory in Fengxian District, Shanghai was used as the culture substrate. Under the microscope, the main characteristics of *Microcystis sp.*cultured in wastewater were chlorophyll-a (Chla) of 2533 mg/m^3, and the density of algae was about 2×10^9 cells/mL. The size of algal cells was 10˜400 μm, and they were clumped.

2.2 The device of microbubble air flotation test

The microbubble air flotation equipment is composed of microbubble generating device and air floating column. Among them, the microbubble generation device is composed of gas-liquid mixing pump (Nikuni, 20 FPD04Z, flow rate: 0.9 m^3/h), the water inlet tank (plexiglas, length × width × height =200×200×500 mm^3, thickness =5 mm) and the dissolved gas tank (stainless steel cylindrical tank, diameter =110 mm, height =810 mm,). The air floating column (length × width × height =100×30×500 mm^3) is made of plexiglas with the thickness of 3 mm. It has good light transmittance and is convenient for dynamic observation of microbubbles. Each part of the test device is connected by PVC pipe (φ=25mm), and the pressure reducing valve is installed between the microbubble generation device and the air floating column. The design of flexible pipe joint is adopted among the above three parts, and the distance between the pressure reducing valve and the air floating column is adjusted by changing the length of the release pipe. The whole test device is also equipped with pressure gauge, gas gauge and flowmeter, which show the dissolved air pressure, inlet air flow rate and inlet water flow rate, respectively. The flow chart of the test device is shown in Figure 1, with the red arrow indicating the flow direction.

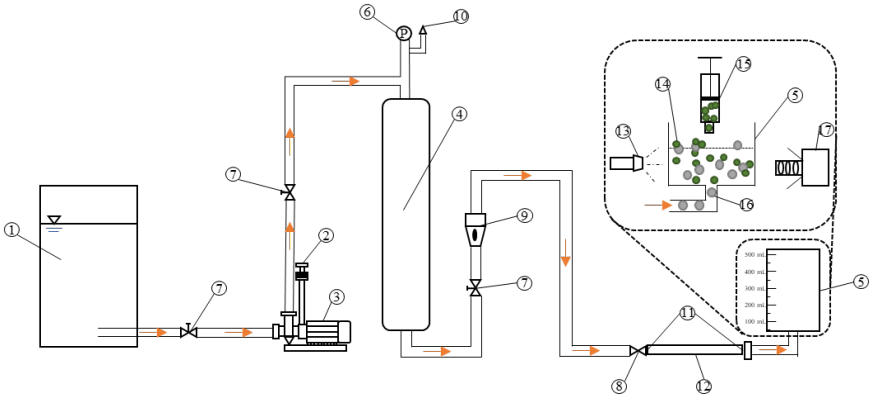

Figure 1 Flow chart of test equipment (1) Reservoir (2) Gasometer (3) Gas-liquid mixing pump (4) Dissloved air vessel (5) Air flotation column (6) Pressure gage (7) Valve (8) Relief valve (9) Flowmeter (10) Safety valve (11) Union (12) The release pipe (13) Light source (14) Microalgae (15) injector (16) bubble (17) high-speed camera)

2.3 Study on the morphology and motion of microbubbles under different parameters

A. **Operational parameters.** Three operational factors including pressure, gas-liquid ratio and length of the release pipe were selected for orthogonal test (3×3) to determine their effects on the particle size of microbubbles. The specific working conditions are shown in Table 1. The test process is as follows: The microbubble air flotation equipment was set and operated in turn under 9 kinds of condition according to Table 1. (1) Start the device. When the liquid level reaches H=400 mm, the high-speed photography system is started to shoot the rising process of microbubbles near H=400 mm. Stop flooding when the liquid level rises to H=450 mm, and the shooting time is 60s. (2) Clean the device. After one shooting, open the drainage valve at the bottom of the air floating column to drain the water, and start the device again to clean the air floating column, so as not to affect the following test results. The dynamic video was observed, and the particle size of bubbles was measured and counted. The proportion of bubbles with particle size [?]50 μm was taken as the experimental index to clarify the relationship between the main factors and the microbubble particle size distribution and obtain the optimal working condition.

Table 1 The orthogonal experiment table

Condition number	A: Pressure /MPa	B: Gas-liquid ratio B/%	C release pipe's length /cm
1	0.55	6	100
2	0.55	5	50
3	0.55	8	10
4	0.45	6	50
5	0.45	5	10
6	0.45	8	100
7	0.35	6	10
8	0.35	5	100
9	0.35	8	50

B. **The diameter of the release pipe.** On the premise of determining the optimal working condition, change the diameter of the release pipe (20, 25, 32 mm) and conduct the test (the test process is the same as A). The influence of the diameter of the release pipe on the particle size distribution of microbubbles was clarified, and the diameter of the release pipe when the particle size of microbubbles was concentrated was

determined.

C. **The shape of the release pipe (straight or elbow).** Select the optimal parameters determined in the above tests and set straight type and elbow type release pipe (with the same straight-line length) as the investigation factor for the test (the test process is the same as A). The influence of different types of release pipe on the particle size distribution of microbubbles was analyzed, and the appropriate type of release pipe was selected.

Based on the test results of A, B and C, the optimal operating conditions (pressure, gas-liquid ratio, release pipe's length, diameter, and type) of the device were determined. The dynamic video of the floating process of microbubbles was observed under the optimal conditions. The clear single microbubble and microbubble combination were selected as the capture objects, and the floating process of the capture objects at the same time was tracked. The kinematic parameter curves (velocity, acceleration, and displacement) of the capture objects were obtained by the high-speed photography system. According to the kinematic parameter curve, the motion state of the single microbubble and the combination was analyzed, the correlation between the particle size of the microbubble and the rising rate was revealed, and the relationship between the particle size of the single microbubble, the particle size of the combination and the rising rate was established.

2.4 Study on the dynamic rule of "Adhesion–Depolymerization" between microbubbles and microalgae

The following tests were carried out under the optimal conditions based on the above tests. Firstly, a syringe was used to inject 5 mL wastewater containing *Microcystis* into the air floating column in the upward direction. When the liquid level reached H=400 mm, the high-speed photography system was used to shoot the rising process of microbubbles and microalgae near H=400 mm. The subsequent procedure is the same as 2.3. In the video, the size and number of microbubbles and microalgae was observed, and the adhesion rule between microbubble and microalgae was summarized.

2.5 Optimization ofharvesting performance of microalgae under the regulation of microbubble flotation

(1) Performance of microbubble flotation for harvesting microalgae under different conditions

According to the results of 2.3 and 2.4, the length of the release pipe was the main influencing factors, the following tests were carried out under different working conditions with the length of the release pipe of 10 cm (condition 1), 25cm (condition 2), 50 cm (condition 3), 75 cm (condition 4), and 100 cm (condition 5), respectively (Table S1). The concentration of Chla of the wastewater which contained*Microcystis* was firstly analyzed. Then the flotation device was installed. 400 mL *microcystis* -containing wastewater was prepared and transferred to the floating column. Start the device and stop the water inlet when the liquid level raised to H =450 mm. The air floating time is 60s. After that, the algal residue was scraped from the top of the air floating column, and the remaining water sample was removed from the bottom of the air floating column. 100 mL of the remaining water sample was used to determine the concentration of Chla after air flotation. After the completion of the first air flotation, open the drainage valve at the bottom of the air flotation column to drain the water, and start the device again to clean the air flotation column, so as not to affect the test results. The above steps were repeated 3 times under the same condition. When the experiment under different conditions was complete, the recovery rate of air flotation was defined based on the change of chlorophyll a concentration before and after flotation. The harvesting performance of the microbubble flotation system under different working conditions was compared and analyzed.

(2) Effects of microalgae densities on the harvesting performance of microbubble flotation

According to the results of experiment (1), the optimal condition was selected, and the experimental device was adjusted accordingly. The mixture with different microalgae density were prepared as following: 400, 800, 1200, 1600 and 2000 mL of microalgae containing wastewater were put into five large beakers, respectively. Then 1600, 1200, 800, 400 and 0 mL of fresh wastewater was added into different beakers to form

a concentration gradient of 1:2:3:4:5, numbered 1˜5 respectively. Then the concentration of Chla in different beakers was determined. The remaining liquids of each beaker were divided into 3 parts with 400 mL volume each. The flotation experiments of different microalgae density were conducted as described above. According to the change of Chla concentration, the effect of algae density on the harvesting performance was investigated.

2.6 Methods

2.6.1 Determination method

See Supporting Information for the determination of microbubble size and microbubble-algal size. The content of chlorophyll a was determined by spectrophotometry.

Algal recovery (%) = (C1-C2) /C1*100

C1: Chla concentration before air flotation (since the ratio of algal water to dissolved air water is 1:2, the Chla concentration before air flotation is 1/3 of the Chla concentration of the original water sample); C2: Chla concentration after air flotation.

2.6.2 Data analysis

The proportion of bubbles with particle size [?]50 μm is selected as the test index to analyze the orthogonal experiment results. With the test index as the dependent variable, and pressure, gas-liquid ratio, and length of the release pipe as fixed factors, SPSS19.0 analysis software is used to analyze the orthogonal experiment results of variance analysis and the effects of key process parameters on the micro bubbles.

3. Result and Discussion

3.1 Influence of key process parameters of air flotation device on microbubble morphology

3.1.1 Morphological characteristics of microbubbles under different process parameters

Smaller bubbles have a higher surface area to volume ratio, which leads to higher probabilities of collision and attachment, a lower detachment probability, lower ascending rate and higher free surface energy (Garg et al., 2014; Hanotu et al., 2012). The optimal bubble size has been reported as approximately 50 μm, and efficiency drops significantly with larger bubbles (Cassell et al., 1975). This was attributed to the reduced number of bubbles, and thus each bubble is required to remove more cells resulting in decreased efficiency (Henderson et al., 2008). Thus, the proportion of microbubbles within 50 μm was analyzed.

The effects of pressure, gas-liquid ratio, and length of the release pipe on the particle size of microbubbles are shown in Table 2. The particle size of the microbubbles produced under the working condition 2/3/4/5/7 are all within 100 μm, and the proportion of microbubbles within 50 μm is more than 74%. The highest (80.58%) was obtained under working condition 2. On the contrary, the particle size of microbubbles produced by working condition 1/6/8/9 exceeds 100 μm, and more than 50% of the microbubbles have a particle size greater than 50 μm. In particular, the particle size distribution range of the microbubbles produced under working condition 6 is the widest, with more than 80% of the microbubbles exceeding 50 μm in size. When the length of the release pipe is 10 cm, that is, working condition 3/5/7, the proportion of microbubbles [?]50 μm is more than 74%; When the length of the release pipe is 100 cm, i.e., working condition 1/6/8, the proportion of microbubbles [?]50 μm is less than 41%.

Table 2 Results of particle size distribution of microbubbles

Condition number	Pressure A/MPa	Gas-liquid ratio B/%	Length of the release pipe C/cm	Proportion of microbubb
1	0.55	6	100	40.97
2	0.55	5	50	80.58
3	0.55	8	10	76.50
4	0.45	6	50	74.95

Condition number	Pressure A/MPa	Gas-liquid ratio B/%	Length of the release pipe C/cm	Proportion of microbubb
5	0.45	5	10	78.45
6	0.45	8	100	19.42
7	0.35	6	10	74.76
8	0.35	5	100	39.81
9	0.35	8	50	39.03

As shown in Fig. 2, the frequency distribution of microbubbles particle size under 9 working conditions concentrated in the range of 35˜45 μm and 55˜70 μm. The particle size of the microbubbles produced in condition 2/3/4/5/7 is concentrated in the front segment, while the particle size of the microbubbles produced in condition 1/6/8/9 is concentrated in the rear segment. The main difference between the two groups mainly lies in the length of the release pipe (10 cm VS 100 cm). The closer the distance between the pressure reducing valve and the air floating column, the shorter the residence time of the released microbubbles in the pipeline. On the one hand, the collision and merger between the microbubbles are reduced. On the other hand, the microbubble movement pressure loss is small. The above two aspects make the microbubbles more stable and the particle size distribution range is narrow.

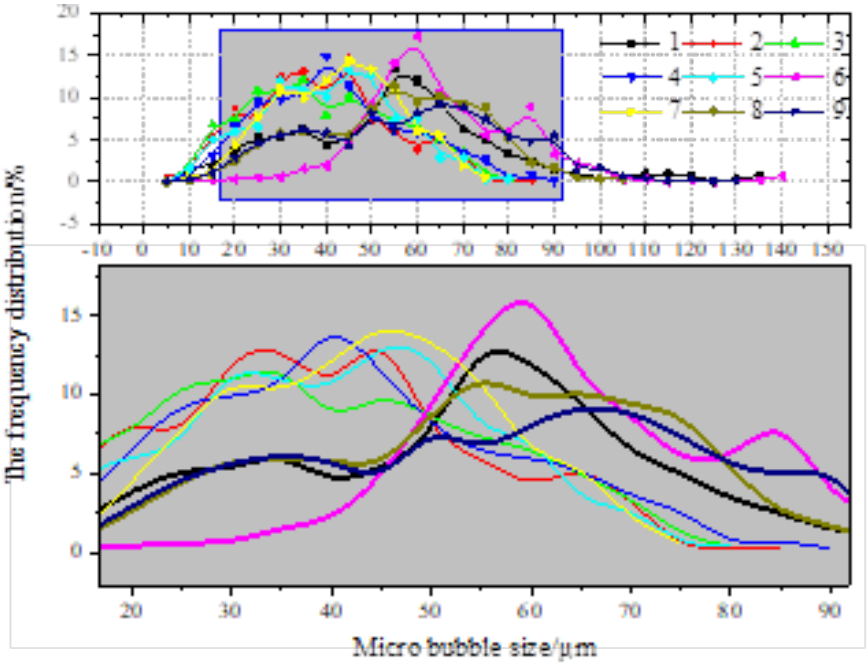

Figure 2 Frequency distribution of microbubble size under nine different conditions

The range analysis of the results shows that the optimal level of each factor is 0.55 MPa of the pressure, 5% of the gas-liquid ratio and 10 cm of the length of the release pipe. The order of the range values of the three factors for the test indexes was length of the release pipe (43.17) > gas-liquid ratio (21.29) > pressure (14.82). The length of the release pipe shows obvious influence on the microbubbles with particle size less than 50 μm in the floating system. The P values of pressure, gas-liquid ratio and length of the release pipe were 0.35, 0.18 and 0.05, respectively. As can be seen from the F-test results, when the confidence level is 95%, only the length of the release pipe is significant to the test index, and there is no significant difference in the influence of pressure (0.35, 0.45, 0.55MPa) and gas-liquid ratio (5%, 6%, 8%) on the test index.

3.1.2 Influence of diameter and shape of the release pipe on the morphological characteristics of microbubbles

The effect of the diameter of the release pipe on the particle size distribution of microbubbles was further explored. It can be seen from Fig. 3 that when the diameter of the release pipe (25 cm) is the same as the pipe, the particle size of microbubbles is concentrated between 20 to 60 μm, and the peak value of the curve appears at 40 μm. When the diameter increased to 32 cm, the particle size distribution curve of microbubbles shifted slightly to the right (20˜70 μm), and the peak value appeared at 45 μm. When the diameter of the release pipe decreased to 20 cm, the particle size distribution curve moved to the right, and the peak value appeared at 60 μm, and the range of the particle size became larger (20˜100 μm). According to the cumulative frequency distribution of bubble size (Fig. 3 (b)), the distribution proportion of microbubbles with particle size less than 50 μm is 35% (diameter=20 cm), 71% (diameter=25 cm) and 67% (diameter=32 cm), respectively.

In conclusion, when the diameter of the release pipe is the same as that of the pipe, the proportion of microbubbles with particle size within 50 μm is the largest, and the particle size distribution is concentrated. This is because when the dissolved air water is released at the pressure reducing valve, the diameter of the release pipe increases, which weakens the turbulence intensity, the spatial density of microbubbles is relatively reduced, the collision rate between microbubbles is reduced, and the microbubbles are relatively stable. However, when the diameter of the release pipe decreases, the resistance of the microbubbles along the path increases, and the pressure loss of the microbubbles is great. At the same time, the spatial density of the microbubbles increases relatively, and the collision probability between the microbubbles increases, leading to the merger or rupture of some microbubbles. Both lead to the larger particle size of the microbubbles.

Hosted file

`image3.emf` available at https://authorea.com/users/758355/articles/732202-application-of-microbubble-air-flotation-to-harvest-microcystis-sp-from-agriculture-wastewater-the-regulation-and-mechanisms

Figure 3. Effect of the diameter and type of the release pipe on the particle size distribution of microbubbles

The size distribution of microbubbles in straight and bend pipes with the same length was shown in Fig. 3(C). The particle size of microbubbles in the straight release pipe is concentrated between 20˜60 μm, and the peak value appears at 40 μm. While the microbubbles generated in the bend pipes are concentrated in 40˜80 μm, and the peak frequency distribution is 55 μm. The cumulative curve of microbubble particle size shows that the proportion of microbubbles with particle size less than 50 μm (65%) generated in the straight release pipe is 20% higher than that of the bend type (Fig. 3(D)). In conclusion, the microbubbles generated by the straight release pipe have small particle size and concentrated distribution range. When the microbubble moves in the straight pipe, it is only subject to the resistance along the way, while when it moves in the release pipe with an elbow, it is also subject to the local resistance generated by the elbow in addition to the resistance along the way, resulting in the loss of microbubble pressure in the pipe, making the microbubble particle size larger. Besides, the elbow increases the turbulence intensity of the fluid, which increases the collision probability in the process of microbubble movement, resulting in the rupture or merger of microbubbles, and the particle size of microbubbles becomes larger.

3.1.3 The relationship between microbubble size and its floating rate

Bubble size was also said to determine the shape and rise pattern of the bubbles (Edzwald, 2010; Eskanlou et al., 2018).The microbubbles (11.29 [?] bubble size [?] 86.19μm, average bubble size = 42.83 μm) generated under the conditions of pressure of 0.45 MPa, gas-liquid ratio of 5 % and release pipe of 10 cm were photographed. A single microbubble with bubble size = 45.19 μm and a combination of two microbubbles with D_b = 65.0 μm (50.97 + 52.19) were selected as targets for dynamic tracking (948 sec˜1009 sec). The target is shown in Fig.S2. (Note: D_b is calculated based on the total volume of the two small microbubbles,

the same below)

The target microbubbles were observed and analyzed during the tracking period to obtain their acceleration curve (Fig. S3 and S4). Fig.S4(A) and (B) represent the acceleration of a single microbubble and a combination of two microbubbles, respectively. The acceleration detection curve reflects the movement of the target throughout the tracking period. The positive and negative in the acceleration detection curve indicate the direction of the acceleration of the target, and the value indicates the magnitude of its acceleration. By comparing and analyzing the acceleration of the single microbubble and the target of the combination, it is found that the acceleration of the two fluctuates regularly. Whether it is a single microbubble or a combination of two microbubbles, the magnitude and direction of the acceleration change throughout the tracking period, which indicates that the resultant force of the microbubble during the floating process is a variable force, and the microbubble performs variable acceleration motion.

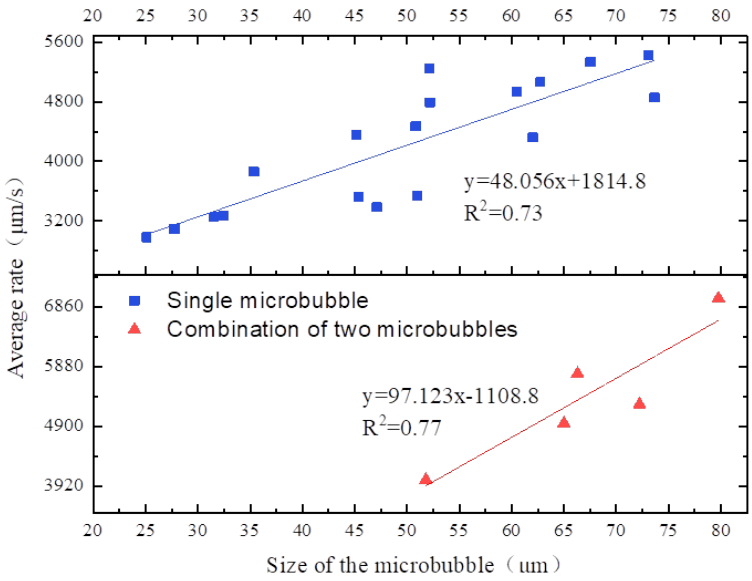

Figure 4 The relationship between microbubble size and its floating rate

The relationship between the particle size and the average rising rate is shown in Fig.4. As the particle size of the microbubbles increases, the average rate increases. The relationship between the average rate and the particle size of a single microbubble is y = 48.056x + 1814.8 (R^2=0.73), and the relationship between the average rate and the particle size of two microbubbles is y=97.123x-1108.8 (R^2=0.77). From the correlation coefficient R^2, in the same water flow environment, whether it is a single microbubble or a combination of two microbubbles, its average rate is positively correlated with its particle size, and the effect of microbubble particle size on the average rate is extremely significant.

3.2 Adhesion efficiency and adhesion mechanism of microbubbles to microalgae

3.2.1 Adhesion mode of microbubble-algae aggregates

The adhesion of microbubbles to algae aggregates is shown in Fig. S5. The adhesion modes of microbubbles to algae include 1-1 (single bubble-single algae), 2-1 (double bubble-single algae), n-1 (multi-bubble-single algae) and n-n (multi-bubble-multi-algae). The first two adhesion modes have one thing in common, that is, algae aggregates are adhered to the lower half of the microbubbles. According to the theory of the interaction between microbubbles and particles, this is because during the floating process of microbubbles, tangential flow is formed around the microbubbles, so that the particles (algae aggregates) adhered to them are gathered in the lower half of the microbubbles.

Due to the high density of algae in the experimental water sample (10^9/ mL), the algae cells in the water sample exist in the form of algae aggregates, and it is difficult to count when the microbubbles adhere to the algae aggregates in the n-n way. Therefore, only the proportion of three adhesion modes of 1-1, 2-1 and n-1 was counted (sample number 1000). When microbubbles adhered to*Microcystis* , the 1-1 mode accounted for 94.6%, the 2-1 mode accounted for 4.7%, and the n-1 mode accounted for less than 1%. When microbubbles adhere to *Microcystis* , the main adhesion mode is 1-1, that is, one microbubble adheres to one algae cell most easily.

3.2.2 Size distribution of microbubble and Microcystis

When the microbubbles adhere to *Microcystis* , the size distribution of microbubble-algae aggregates is shown in Fig.5. The particle size of microbubbles in the microbubble-algae complex was in the range of 10˜170 μm, and the size of*Microcystis* was in the range of 10˜400 μm. Among them, the proportion of microbubbles with a particle size of 70˜125 μm is as high as 87%, and 85% of*Microcystis* are concentrated in 50˜200 μm. In the size-frequency distribution curve of adhered *Microcystis* (Fig. 5(b)A), the peak frequency of *Microcystis* appeared at 100 μm (8.5%), that is, *Microcystis* in the range of 90˜100 μm accounted for 8.5% of the total*Microcystis* . In the particle size distribution curve of microbubbles (total microbubbles) adhering to *Microcystis* (Fig. 5(b)B), the peak frequency of microbubble size appeared at 90 μm (12.0%), that is, microbubbles with particle size between 80˜90 μm accounted for 12.0% of the total microbubbles. In the particle size distribution of microbubbles generated under this working condition (see Fig. 5(b)C), 45.8% of the microbubbles were distributed between 40 and 60 μm, and the proportion of microbubbles adhering to *Microcystis* (80˜90 μm) was less than 1%. The frequency distribution peak of the particle size of the adhered microbubbles is like that of the microalgae. It was reported that morphology of algae including shape and size also have impacts on the performance of flotation process when considering the bubble-cell attachment, in addition, spherical (*Microcystis*) and oval (*Chlamydomonas*) configures had greater flotation efficiencies than filamentous shape (*Phormidium*) (Bui et al., 2015).

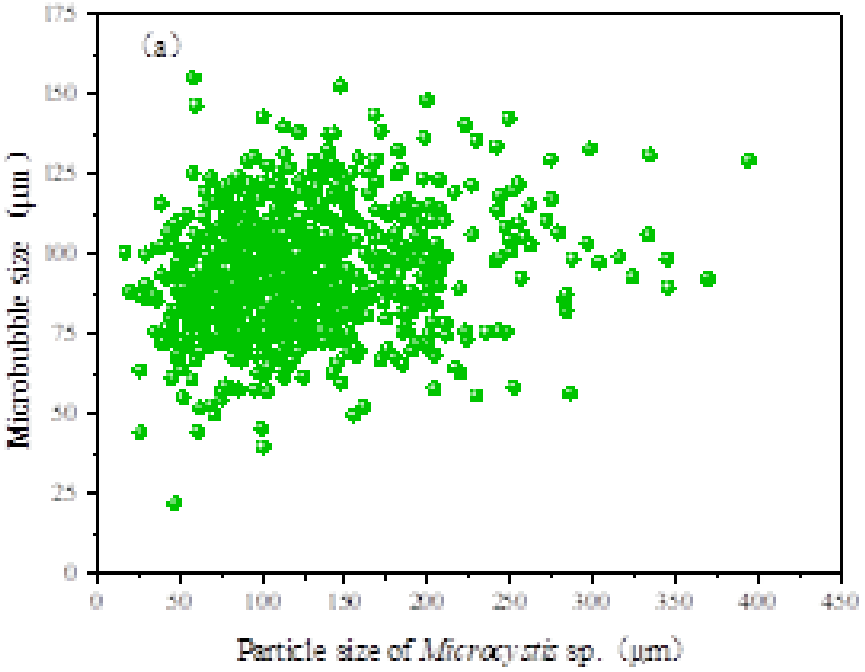

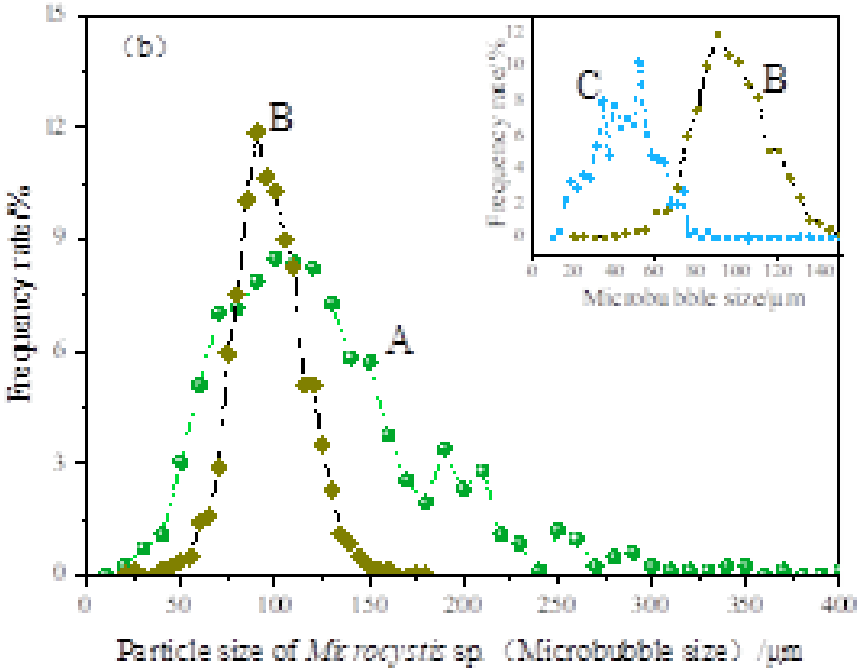

Figure 5 (a) Distribution curve of microbubble size and *Microcystis* sp. Size (b) Distribution curve of microbubble size and *Microcystis* sp. frequency

3.2.3 Response relationship between microbubble size and Microcystis size

The particle size ratio distribution of adhered *Microcystis* and microbubbles is shown in Fig.6 A). The particle size ratio of*Microcystis* and microbubbles is in the range of 0˜4.2. When the ratio of the two is between 0 and 1.2, with the increase of the ratio, the proportion of microbubble-Microcystis in this range increases from 0.5% to 22.1%. When the ratio increases from 1.2 to 4.2, the proportion of microbubble-Microcystis in this range gradually decreases. With the ratio exceeding 2.7, the proportion is less than 2%. From the cumulative percentage, the cumulative ratio in the range of 0.6˜1.5 is as high as 63%, and the cumulative curve rises slowly when the ratio is greater than 1.5. When the size of*Microcystis* is 0.6˜1.5 times the size of microbubbles, *Microcystis* is easily adhered by microbubbles, and the adhesion rate is as high as 63%. Among them, the probability of adhesion is the highest when the ratio is between 0.9˜1.2.

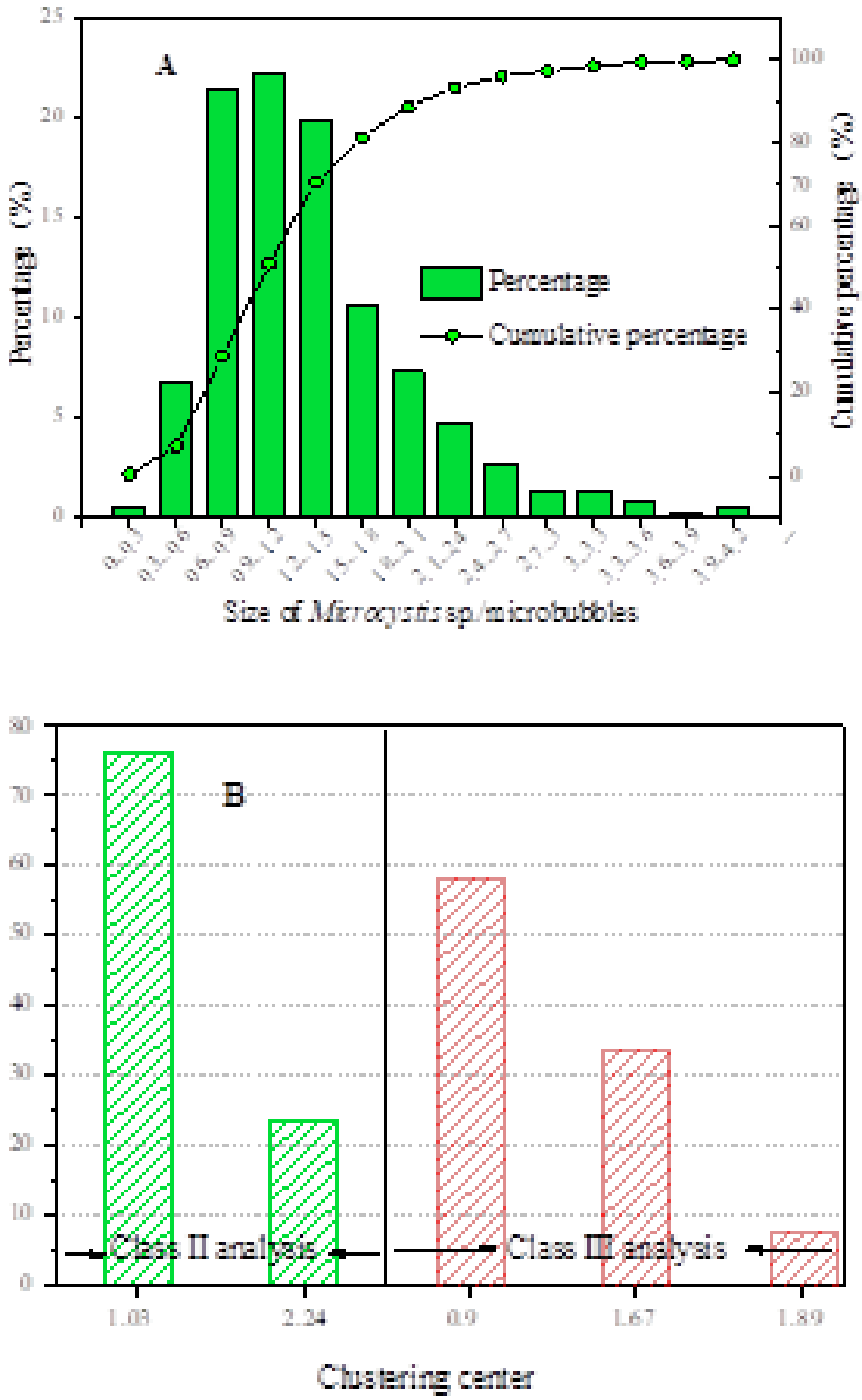

Figure 6. (A) ratio of *Microcystis* sp. size to microbubble size; (B) cluster analysis of *Microcystis* sp. and microbubble particle size

The cluster analysis results of the size ratio of *Microcystis* and microbubble are shown in Fig. 6(B). Class II analysis were carried out and the clustering centers were 1.03 and 2.24. The proportion of cases in each clustering center was 76% and 23%, respectively. The cluster centers of the Class III analysis were 0.9,1.67

and 2.89, accounting for 58%, 34% and 8%, respectively. Based on the results of the two types of analysis, it is known that in the formed microbubble-algae combination, the proportion of Microcystis/microbubble size ratio of 1.03 and 0.9 is the highest, and both exceed 50%. When the size of*Microcystis* is equivalent to the size of microbubbles, the two are most likely to adhere.

3.3 Effects of the microbubble flotation parameters on microalgae harvest performance

The performance of microbubble air flotation on *Microcystis*harvesting under different working conditions is shown in Fig.7(A). The concentration of Chla was 844 mg/m^3 before air flotation, and the concentration of Chla decreased significantly after microbubble air flotation. Among them, the lowest Chla concentration after flotation in condition 5 was 308 mg/ m^3, and the highest Chla concentration after flotation in condition 1 was 532 mg/m^3. The recovery rate of *Microcystis* by microbubble air flotation under different working conditions was sorted from high to low as follows: working condition 5 (63.5%) > working condition 4 (52%) > working condition 2 (50%) > working condition 3 (41%) > working condition 1 (37%). According to the content of 3.2.1, the distribution peak of *Microcystis* is 90˜100 μm, and the adhesion rate is the largest when the particle size of microbubbles is equal to the size of *Microcystis* . The proportion of bubbles with a particle size greater than 80 μm produced by condition 5 is the largest, and its algae harvesting efficiency is the highest. The proportion of bubbles with a particle size of more than 80 μm produced by condition 1 is the smallest, and its algae collection rate is the lowest. The proportion of bubbles with a particle size of more than 80 μm produced by condition 3 is greater than that of condition 2, but its algae collection efficiency is 9% lower than that of condition 2, which may be caused by the floating of multiple large bubbles observed during the experiment. Because the fast-floating speed of large bubbles disturbed the adhesion of microbubbles to the algae, or caused the desorption of the microbubble-microcystin aggregates that have adhered, thereby reducing the algae collection rate. In the process of harvesting algae by microbubble air flotation, the rate of algae harvesting depends not only on the adhesion of microbubbles to algae, but also on the influence of water flow environment.

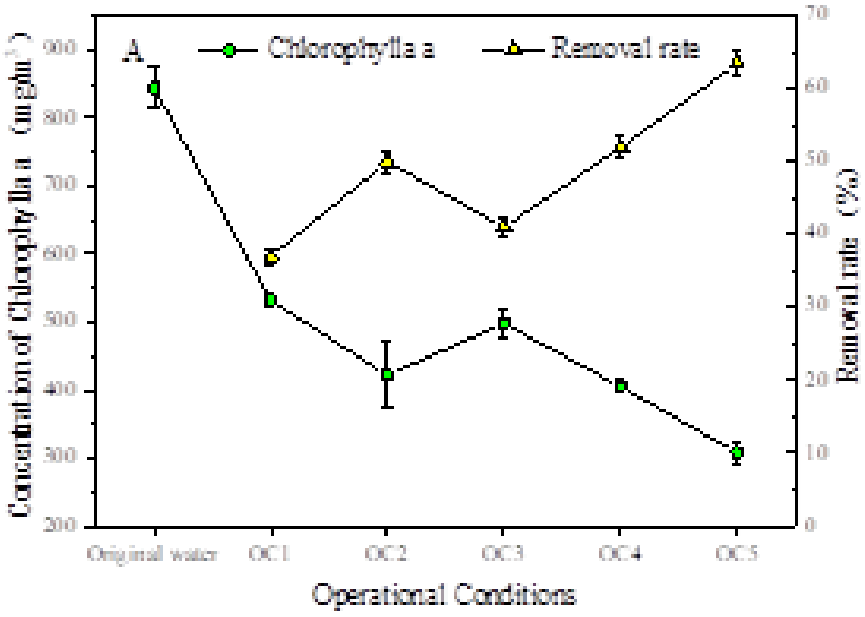

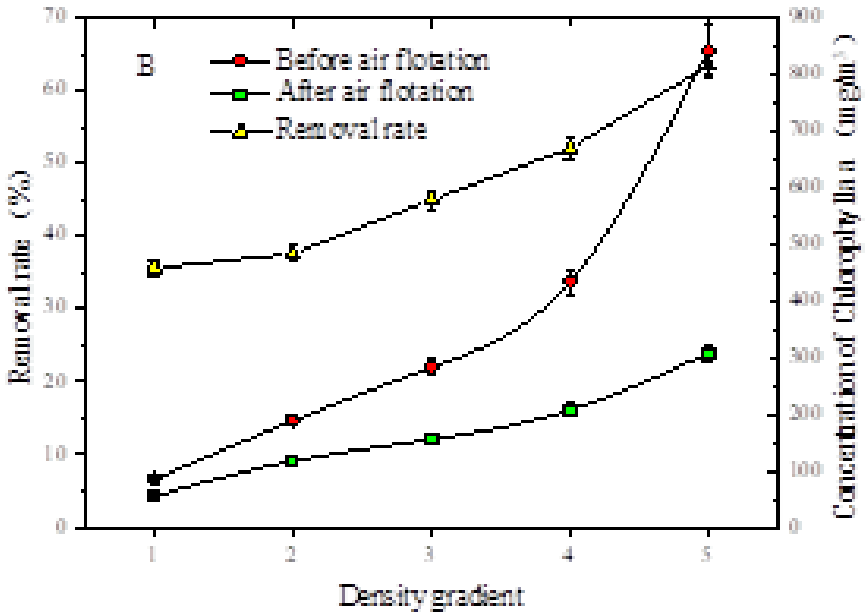

Fig. 7 Effect of micro-bubbles flotation on *Microcystis* sp. harvesting under different conditions(A) and density(B)

The results of microbubble air flotation treatment of *Microcystis*with different density under the condition of condition 5 are shown in Fig. 7(B). It can be seen from the diagram that with the increase of Chla concentration from 85 mg/m^3 to 844 mg/m^3, the recovery rate of microbubble air flotation to *Microcystis* also showed an increasing trend. After flotation, the Chla concentration of density 1 decreased to 54 mg/m^3, and the Chla concentration of density 5 decreased to 126 mg/m^3. The lowest algae collection rate of microbubble air flotation for density 1 was 35.6%, while the algae collection rate for density 5 was as high as 63.5%. The analysis shows that under low concentration conditions, the number of*Microcystis* colonies is small, and the probability of adhesion by microbubbles is small; when the algae concentration increased to 844 mg/m^3, the number of *Microcystis* colonies in the water increased, the probability of microbubbles colliding with them increased, and the adhesion probability also increased. Microbubble air flotation has a better harvesting effect on higher *Microcystis*density.

4.Conclusion

Microbubble air flotation is an effective way for microalgae harvesting. During the process of microbubble generation, the proportion of microbubbles with particle size less than 50 μm is optimal with the pressure of 0.55 MPa, the gas-liquid ratio of 5 % and the length of the release pipe of 10 cm, and the length of the release pipe is the main influencing factor, followed by the gas-liquid ratio. No matter a single microbubble or a combination of two microbubbles, they all undergo variable acceleration motion during the floating process. In the process of adhesion, when the size of *Microcystis* was 0.6˜1.5 times of the size of microbubbles, microbubbles could adhere to 63% of*Microcystis* . When the size of *Microcystis* was equivalent to the size of microbubbles (ratio of 1.03 to 0.9), the adhesion probability of the two was the largest (both more than 50%). That can also explain that the best the harvesting rate of *Microcystis* (63.5%) was obtained under the working condition 5 (pressure 0.45 MPa, gas-liquid ratio 5% and length of the release pipe 100 cm) due to the similar size distribution of the microbubbles and the *Microcystis* in this study. The harvesting performance was also affected by the*Microcystis* density and the water flow environment. More investigations would need to be undertaken for application in large scale with varied concentrations and other dissolved organic matters.

Acknowledgement

This work was financially supported by the Key Technologies Research and Development Program (2017YFE0135500); the National Natural Science Foundation of China (51908355); the Natural Science Foundation of Shanghai (19ZR1443700); and the Scientific and Innovative Action Plan of Shanghai (19DZ1204500).

References

Ali, S., Paul Peter, A., Chew, K. W., Munawaroh, H. S. H., & Show, P. L. (2021). Resource recovery from industrial effluents through the cultivation of microalgae: A review. *Bioresource Technology* ,*337* , 125461. https://doi.org/10.1016/j.biortech.2021.125461

Aravani, V. P., Sun, H., Yang, Z., Liu, G., Wang, W., Anagnostopoulos, G., & Papadakis, V. G. (2022). Agricultural and livestock sector's residues in Greece & China: Comparative qualitative and quantitative characterization for assessing their potential for biogas production.*Renewable and Sustainable Energy Reviews* , *154* , 111821. https://doi.org/10.1016/j.rser.2021.111821

Aulenbach, D. B., Shammas, N. K., Wang, L. K., & Marvin, R. C. (2010).*Algae removal by flotation* . Humana Press.

Bui, T. T., Nam, S.-N., & Han, M. (2015). Micro-bubble flotation of freshwater algae: A comparative study of differing shapes and sizes.*Separation Science and Technology* , *50* (7), 1066-1072. https://doi.org/10.1080/01496395.2015.1005313

Cassell, E. A., Kaufman, K. M., & Matijevic, F. (1975). The effects of bubble size on micro-flotation. *Water Research* , *9* , 1017-1024.

Christenson, L., & Sims, R. (2011). Production and harvesting of microalgae for wastewater treatment, biofuels and bioproducts.*Biotechnology Advances* , *29* , 686-702. https://doi.org/10.1016/j.biotechadv.2011.05.015

Edzwald, J. K. (2010). Dissolved air flotation and me. *Water Research* , *44* (7), 2077-2106. https://doi.org/10.1016/j.watres.2009.12.040

Eskanlou, A., Khalesi, M. R., Mirmogaddam, M., Hemmati Chegeni, M., & Vaziri Hassas, B. (2018). Investigation of trajectory and rise velocity of loaded and bare single bubbles in flotation process using video processing technique. *Separation Science and Technology* ,*54* (11), 1795-1802. https://doi.org/10.1080/01496395.2018.1539104

Fasaei, F., Bitter, J. H., Slegers, P. M., & van Boxtel, A. J. B. (2018). Techno-economic evaluation of microalgae harvesting and dewatering systems. *Algal Research* , *31* , 347-362. https://doi.org/10.1016/j.algal.2017.11.038

Fuad, N., Omar, R., Kamarudin, S., Harun, R., Idris, A., & Wan, A. W. A. K. G. (2018). Mass harvesting of marine microalgae using different techniques. *Food and Bioproducts Processing* , *112* , 169-184. https://doi.org/10.1016/j.fbp.2018.10.006

Garg, S., Wang, L., & Schenk, P. M. (2014). Effective harvesting of low surface-hydrophobicity microalgae by froth flotation. *Bioresource Technology* , *159* , 437-441. https://doi.org/10.1016/j.biortech.2014.03.030

Hanotu, J., Bandulasena, H. C. H., & Zimmerman, W. B. (2012). Microflotation performance for algal separation. *Biotechnology and Bioengineering* , *109* , 1663-1673. https://doi.org/10.1002/bit.24449

Henderson, R. K., Parsons, S. A., & Jefferson, B. (2008). Surfactants as bubble surface modifiers in the flotation of algae: Dissolved air flotation that utilizes chemically modified bubblesurface.*Environmental Science & Technology* , *42* , 4883-4888. https://doi.org/10.1021/es702649h

Laamanen, C. A., Desjardins, S. M., Senhorinho, G. N. A., & Scott, J. A. (2021). Harvesting microalgae for health beneficial dietary supplements. *Algal Research* , *54* , 102189. https://doi.org/10.1016/j.algal.2021.102189

Lopez-Sanchez, A., Silva-Galvez, A. L., Aguilar-Juarez, O., Senes-Guerrero, C., Orozco-Nunnelly, D. A., Carrillo-Nieves, D., & Gradilla-Hernandez, M. S. (2022). Microalgae-based livestock wastewater treatment (MbWT) as a circular bioeconomy approach: Enhancement of biomass productivity, pollutant removal and high-value compound production. *Journal of Environmental Management* , *308* , 114612. https://doi.org/10.1016/j.jenvman.2022.114612

Molina, G. E., Belarbi, E. H., Acie´n Ferna´ndez, F. G., Robles, M. A., & Chisti, A. (2003). Recovery of microalgal biomass and metabolites: Process options and economics. *Biotechnology Advances* , *20* , 491-515. https://doi.org/10.1016/S0734-9750(02)00050-2

Oh, H. M., Lee, S. J., Park, M. H., Kim, H. S., Kim, H. C., Yoon, J. H., & Yoon, B. D. (2001). Harvesting of Chlorella vulgaris using a bioflocculant from *Paenibacillus sp. AM49* . *Biotechnology Letters* , *23* , 1229–1234. https://doi.org/10.1023/A:1010577319771

Peter, A. P., Koyande, A. K., Chew, K. W., Ho, S.-H., Chen, W.-H., Chang, J.-S., & Show, P. L. (2022). Continuous cultivation of microalgae in photobioreactors as a source of renewable energy: Current status and future challenges. *Renewable and Sustainable Energy Reviews* , *154* , 111852. https://doi.org/10.1016/j.rser.2021.111852

Rawat, I., Kumar, R. R., Mutanda, T., & Bux, F. (2013). Biodiesel from microalgae: a critical evaluation from laboratory to large scale production. *Applied Energy* , *103* , 444-467. https://doi.org/10.1016/j.apenergy.2012.10.004

Rawat, I., Ranjith Kumar, R., Mutanda, T., & Bux, F. (2011). Dual role of microalgae: Phycoremediation of domestic wastewater and biomass production for sustainable biofuels production. *Applied Energy* ,*88* (10), 3411-3424. https://doi.org/10.1016/j.apenergy.2010.11.025

Siddiki, S. Y. A., Mofijur, M., Kumar, P. S., Ahmed, S. F., Inayat, A., Kusumo, F., & Mahlia, T. M. I. (2022). Microalgae biomass as a sustainable source for biofuel, biochemical and biobased value-added products: An integrated biorefinery concept. *Fuel* , *307* , 121782. https://doi.org/10.1016/j.fuel.2021.121782

Teixeira, M. R., Sousa, V., & Rosa, M. J. (2010). Investigating dissolved air flotation performance with cyanobacterial cells and filaments. *Water Research* , *44* (11), 3337-3344. https://doi.org/10.1016/j.watres.2010.03.012

Uduman, N., Qi, Y., Danquah, M. K., Forde, G. M., & Hoadley, A. (2010). Dewatering of microalgal cultures: a major bottleneck to algae-based fuels. *Journal of Renewable and Sustainable Energy* , *2* (1), 012701. https://doi.org/10.1063/1.3294480

Yoro, K. O., Daramola, M. O., Sekoai, P. T., Wilson, U. N., & Eterigho-Ikelegbe, O. (2021). Update on current approaches, challenges, and prospects of modeling and simulation in renewable and sustainable energy systems. *Renewable and Sustainable Energy Reviews* ,*150* , 111506. https://doi.org/10.1016/j.rser.2021.111506

Zhou, H., Ji, C., Li, J., Hu, Y., Xu, X., An, Y., & Cheng, L. (2021). Understanding the interaction mechanism of algal cells and soluble algal products foulants in forward osmosis dewatering. *Journal of Membrane Science* , *620* , 118835. https://doi.org/10.1016/j.memsci.2020.118835